

The Interaction of SWI/SNF with the Ribosome Regulates Translation and Confers Sensitivity to Translation Pathway Inhibitors in Cancers with Complex Perturbations



Livia Ulicna¹, Samuel C. Kimmey^{1,2}, Christopher M. Weber¹, Grace M. Allard¹, Aihui Wang¹, Nam Q. Bui², Sean C. Bendall¹, Gerald R. Crabtree^{1,3}, Gregory R. Bean¹, and Capucine Van Rechem¹

ABSTRACT

Subunits from the chromatin remodelers mammalian SWI/SNF (mSWI/SNF) are mutated, deleted, or amplified in more than 40% of cancers. Understanding their functions in normal cells and the consequences of cancerous alterations will provide insight into developing new targeted therapies. Here we examined whether mSWI/SNF mutations increase cellular sensitivity to specific drugs. Taking advantage of the DepMap studies, we demonstrate that cancer cells harboring mutations of specific mSWI/SNF subunits exhibit a genetic dependency on translation factors and are sensitive to translation pathway inhibitors. Furthermore, mSWI/SNF subunits were present in the cytoplasm and interacted with the translation initiation machinery, and short-term inhibition and depletion of specific subunits decreased global

translation, implicating a direct role for these factors in translation. Depletion of specific mSWI/SNF subunits also increased sensitivity to mTOR-PI3K inhibitors. In patient-derived breast cancer samples, mSWI/SNF subunits expression in both the nucleus and the cytoplasm was substantially altered. In conclusion, an unexpected cytoplasmic role for mSWI/SNF complexes in translation suggests potential new therapeutic opportunities for patients afflicted by cancers demonstrating alterations in their subunits.

Significance: This work establishes direct functions for mSWI/SNF in translation and demonstrates that alterations in mSWI/SNF confer a therapeutic vulnerability to translation pathway inhibitors in cancer cells.

Introduction

The SWI/SNF (mSWI/SNF) complexes are ATP-dependent chromatin remodelers that influence chromatin architecture and gene expression (1–3). The three main human complexes, BAF, PBAF, and ncBAF, are composed of common and specific subunits altered by mutations and copy-number variation in more than 40% of cancers (1, 2, 4). Many mutations result in loss-of-function driving disease progression and therapeutic resistance (1–3, 5).

While mSWI/SNF functions are mostly studied through direct interaction with the nucleosome, few studies investigate nonchromatin substrates. In yeast, SWI/SNF evicts Sir3p from the nucleosome (6), and Brg1 (SMARCA4) activates Mec1 kinase (7). In humans, BAF evicts PRC1 from the chromatin (8). Furthermore, mSWI/SNF subunits shuttle between nucleus and cytoplasm (9, 10). Differential localization could be disease-relevant: SMARCA4 is cytoplasmic in

some corticotroph adenomas (11), nuclear SMARCA2 correlates with better prognosis in lung cancer (12), and cytoplasmic ARID1B promotes oncogenesis and correlates with advanced pancreatic cancer (13). Together, these studies provide evidence for possible disease-associated functions for mSWI/SNF outside roles on the nucleosome.

In this study, we report mSWI/SNF-mutated cancer cell lines' genetic dependency to translation factors and sensitivity to translation pathway inhibitors. We demonstrate mSWI/SNF subunits interact with the translation machinery and affect translation. mSWI/SNF inhibition and depletion in combination with mTOR-PI3K inhibitors decrease cell viability, suggesting a possibility for translation-targeted therapy in mSWI/SNF-perturbed diseases. Indeed, expression of SMARCA4 loss-of-function pathogenic mutations decreases translation. Finally, we reveal the substantial alteration of mSWI/SNF subunits' nuclear and cytoplasmic expression in breast cancers. Together, our data support a direct role for mSWI/SNF in translation with the potential to develop into new therapeutic strategies.

Materials and Methods

Cell culture

HEK293T and HME-1 cells were obtained from ATCC. HAP1—wild-type (WT) and HAP1-SMARCA2 (HZGHC004055c012), -SMARCA4 (HZGHC002878c004), -ARID2 (HZGHC000907c009), -ARID1A (HZGHC000618c010), -BRD7 (HZGHC000923c010), -BRD9 (HZGHC000934c010) knockout (KO) cell lines were obtained from and characterized by Horizon Discovery. Cells were cultivated following supplier's instructions. HAP1 cell lines were used under 30 passages. Mouse embryonic stem cells genome editing and culture are described in ref. 14. Cells were regularly tested for *Mycoplasma* (Mycoalert, Lonza).

¹Department of Pathology, Stanford University, Stanford, California.

²Department of Medicine/Oncology, Stanford University, Stanford, California.

³Department of Developmental Biology, Stanford University, Stanford, California.

Corresponding Author: Capucine Van Rechem, Ph.D. Stanford Medicine Department of Pathology, 269 Campus Drive, CCSR-3245C, Stanford, CA 94305-5176. Phone: 650-723-7698; E-mail: cvrechem@stanford.edu

Cancer Res 2022;82:2829–37

doi: 10.1158/0008-5472.CAN-21-1360

This open access article is distributed under the Creative Commons Attribution-NonCommercial-NoDerivatives 4.0 International (CC BY-NC-ND 4.0) license.

©2022 The Authors; Published by the American Association for Cancer Research

Cell fractionation

Cell fractionation was performed as in ref. 15. For the Western blot analysis a comparable fraction of each compartment was loaded on a gel.

Drugs and antibodies

See supplements.

IHC

The studies were conducted in accordance with recognized ethical guidelines, utilized retrospective tissue samples, and were approved by an institutional review board. The tissue microarray includes a wide range of patient ages, tumor grades, and are composed of estrogen receptor-positive, HER2-positive, and triple-negative cases. It is composed of 46 tumors cases from 2002 to 2019 including primary tumors and nodal and distant metastases. Targeted genomic data are available for these tumors. Clinical information and results are reported in Supplementary Table S1. SMARCA4 was performed on a Roche Ventana Benchmark Ultra instrument using CC1 retrieval and antibody dilution at 1:25. SMARCA2 (1:300), BRD7 (1:400), and PB1 (1:2,000) were performed manually using Tris-EDTA antigen retrieval (pH 9). ARID2 (1:250) was performed manually using citrate antigen retrieval (pH 6). Phospho-RPS6 was performed with VECTASTAIN Elite ABC Universal PLUS kit (Vector Laboratories Inc.) using citrate antigen retrieval (pH 6). Subcellular localizations were identified by comparison with hematoxylin and eosin (H&E) staining from the same samples.

Immunoprecipitation and mass spectrometry

Immunoprecipitation was performed as in ref. 16. +RNase: RNase A (1 µg/mL) was added in the lysates prior to immunoprecipitation. Mass spectrometry (MS) experiments were performed using a nanoAcquity liquid chromatography (Waters) coupled to an Orbitrap Q Exactive HF-X mass spectrometer (Thermo Fisher Scientific). For complete MS protocol and data analysis see supplements.

Proximity ligation assays

Proximity ligation assays were performed were performed following supplier's instructions from Duolink PLA (Sigma Millipore). HEK293T cells were seeded 24 hours prior the experiments to reach a confluency of 80%. Cells were imaged with Leica DM400 objective 40×/1.27.

Polysome profiling

Polysome profiling were performed as in ref. 16. Because of the high number of proteins tested and size restriction, identical fractions from polysome profiles were assessed with several gels. mSWI/SNF inhibitors concentrations: iBRD9 10 µg/ml, PFI-3 5 µmol/L, TP472 5 µmol/L.

Simultaneous overview of trimolecule biosynthesis

Simultaneous overview of trimolecule biosynthesis (SOM₃B) was performed as in ref. 17. Cells were treated with inhibitors, puromycin, IdU, and BrU for 10 minutes. Single-cell mass cytometry datasets are available in flowrepository.org (FR-FCM-Z3XL).

Translation assays

L-Azidohomoalanine (AHA) incorporation were performed as in ref. 16, AHA was added for the last hour of drug treatments. Puromycin incorporation assays were performed as in ref. 18, puromycin was added for the last 30 minutes of drug treatments.

Antibodies intensities from Western blot membranes were analyzed using ImageJ. Because of the string smear obtained for these Western blots, loading controls (actin) were run on separate membranes. Quantification panels represent the average of three independent experiments. mSWI/SNF inhibitors concentrations: iBRD9 10 µg/mL, PFI-3 5 µmol/L, TP472 5 µmol/L.

Viability assays

Viability assays were performed following supplier's instructions from the CellTiter-Glo 2.0 Cell Viability Assay (Promega). Luminescence reading was performed using GloMax Explorer Microplate Reader (Promega). mSWI/SNF and translation pathway inhibitors concentrations (unless annotated): iBRD9 10 µg/mL, PFI-3 5 µmol/L, TP472 5 µmol/L, AZD8055 50 nmol/L, BEZ235 50 nmol/L.

Quantification and statistical analysis

Experiments were performed at least three independent times. Data are expressed as mean ± SEM. *P* values < 0.05 calculated with a two-tailed Student *t* test were considered significant and annotated with “*” or “#.”

Data availability

The data generated in this study are available within the article and its Supplementary data files. Single-cell mass cytometry datasets are available in flowrepository.org (FR-FCM-Z3XL).

Results

Cancer cells harboring mSWI/SNF mutations are sensitive to translation pathway inhibitors and are genetically dependent to translation factors

Analysis of the DepMap PRISM repurposing primary drug sensitivity screen testing 578 cell lines with 4,686 compounds (19) revealed that cells harboring mutations in 11 of 29 mSWI/SNF subunits were more sensitive to inhibitors targeting translation and its pathways when compared with all other cell lines. Further analysis of the DepMap genetic dependency study reporting RNAi against 17,309 genes in 712 cell lines (20) revealed that cells harboring mutations in 15 of 29 mSWI/SNF subunits exhibited genetic dependencies to one or more translation factors. For example, *ARID1A* and *ARID1B* mutated cancer cells were more sensitive to AKT and mTOR/PI3K inhibitors (Fig. 1A; Supplementary Fig. S1A) and were genetically dependent to the ribosomal subunit RPL22L1, the RNA helicases DDX27 and DHX9, and SRSF1, a splicing factor with direct role in translation (Fig. 1B; Supplementary Fig. S1B).

Cytoplasmic mSWI/SNF interacts with the translation machinery

To further understand the unexpected association of mSWI/SNF with translation, we assessed mSWI/SNF subunits subcellular localization. Biochemical fractionation from human embryonic kidney HEK293T cells revealed their substantial presence in the cytoplasm (Fig. 1C). We therefore hypothesized mSWI/SNF could be involved in translation. Immunoblots from polysome profile fractions revealed mSWI/SNF subunits enriched in initiating fractions (Fig. 1D–E; Supplementary Fig. S1C). We confirmed mSWI/SNF interaction with translation factors by coimmunoprecipitation, proximity ligation assays (various intensity of cytoplasmic signal was observed in the vast majority of the cells), and MS (Fig. 1F–H; Supplementary Fig. S1D–S1H). Some subunits such as SMARCA4 were detected in

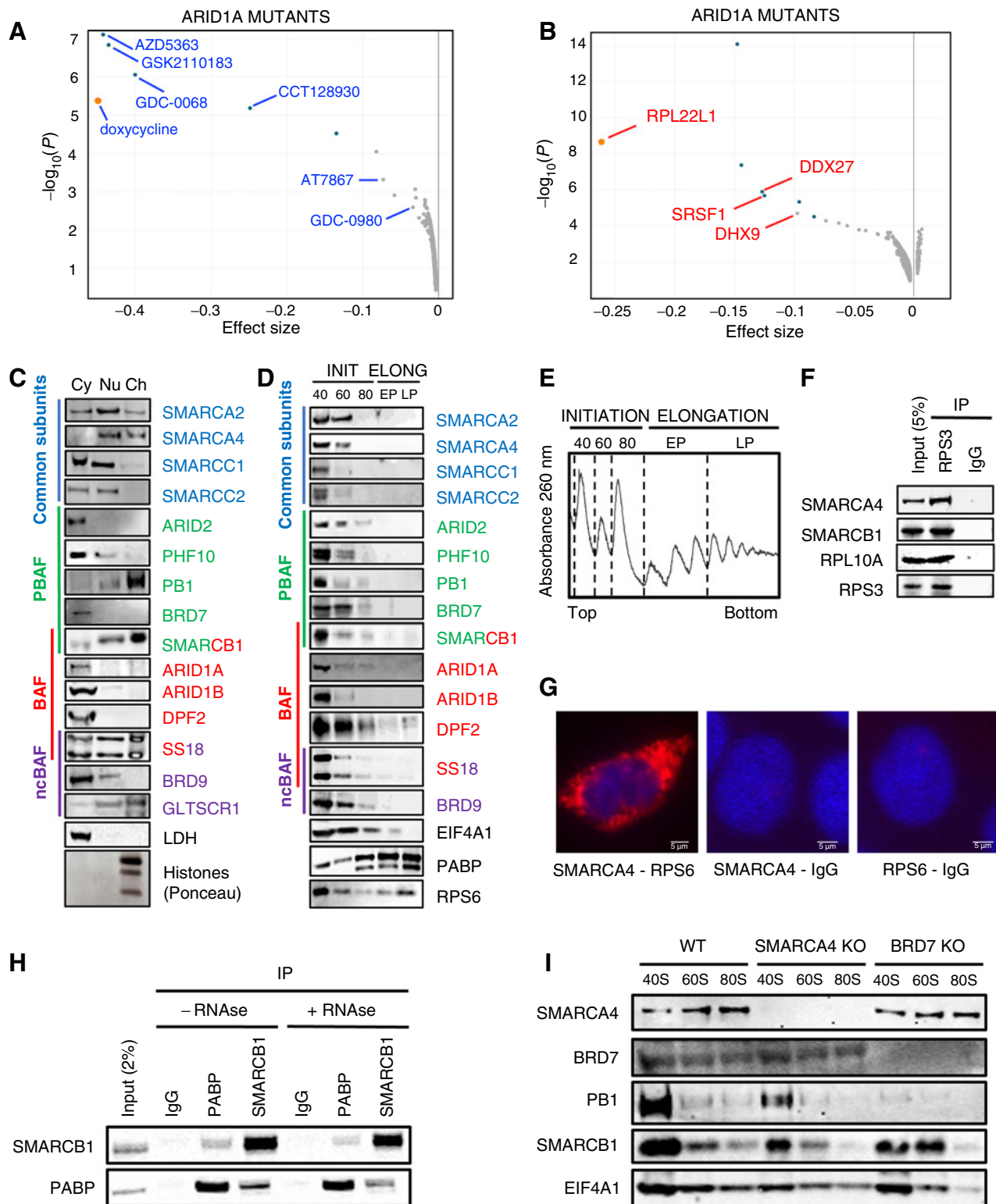


Figure 1.

Cytoplasmic mSWI/SNF interacts with the translation machinery. **A**, Drug sensitivity of ARID1A mutated cancer cells. **B**, Genetic dependency of ARID1A mutated cancer cells. Orange, most prominent translation-related gene/drug. Blue, $q \leq 0.05$. **C**, Fractionated HEK293T. Cy, cytoplasm; Nu, nucleus; Ch, chromatin. **D**, HEK293T polysome profiles fractions. INIT, initiation; ELONG, elongation. **E**, HEK293T polysome profile. **F**, Coimmunoprecipitations from HEK293T. **G**, Proximity ligation assay (PLA) in HEK293T. Immunofluorescence microscopy illustrating a positive PLA signal demonstrating the proximity of SMARCA4 and RPS6 in the cytoplasm (left). Controls with SMARCA4 and a control antibody (middle) or RPS6 and a control antibody (right) do not display PLA signal. **H**, Coimmunoprecipitations from HEK293T. **I**, WT, SMARCA4-, and BRD7-KO HAP1 polysome profiles fractions. EP, early polysomes; IP, immunoprecipitation; LP, late polysomes.

the cytoplasm only upon separation of the translation initiation machinery (Supplementary Fig. S1C compare fractions 1 to 2–4), when performing proximity ligation assays (Fig. 1G), or when enriched by immunoprecipitation (Supplementary Fig. S1D and S1E). Consistent with mSWI/SNF subunits forming complexes (21), deletion of *BRD7* led to the loss of PB1 but not SMARCA4 nor SMARCB1 from initiating fractions (Fig. 1I). These data suggest that mSWI/SNF complexes could directly impact translation.

mSWI/SNF inhibition alters translation

To investigate involvement in translation, we tested mSWI/SNF bromodomain inhibitors (Fig. 2A). A 24-hour treatment decreased translation (Fig. 2B and C) without altering proliferation (Supplementary Fig. S2A). To decipher if these translational defects could be a consequence of direct roles in translation, we shortened treatment to 10 minutes to capture any changes in translation before transcriptional changes would be observed at the protein level, as RNA transcription, export, and translation take at least 20 minutes for small proteins (22, 23). A 10-minute inhibition reduced translation to a similar extent as 24 hours (Fig. 2D). We then performed SOM₃B to measure viability and puromycin and BrU incorporation in single cells (17). We confirmed 10-minute inhibition decreased translation in live cells (Supplementary Fig. S2B–S2C). While we did not detect any changes in transcription (data not shown), 10 minutes is a short timeframe for BrU incorporation and the detected signal was not reliable. Translation remains active during interphase and is reduced during mitosis (24). To assess translation across cell cycle, we examined IdU incorporation, cyclin B1, and histone H3 serine 10 phosphorylation (17). mSWI/SNF inhibition reduced translation across interphase and very modestly in mitosis (Supplementary Fig. S2D–S2E). Finally, we demonstrated that 10 minutes of mSWI/SNF inhibition substantially decreased RPS6 phosphorylation, consistent with a decrease of translation (Fig. 2E; ref. 25).

We then assessed translational defects by polysome profiling. Inhibition for 24 hours increased 80S and decreased polysomes, typical of a translation initiation defect. Inhibition for 10 minutes increased polysomes, which could be reflective of ribosome collision (Fig. 2F; Supplementary Fig. S2F–S2I).

Because mSWI/SNF inhibition decreased translation, we hypothesized mSWI/SNF inhibitors could increase cells' sensitivity to translation inhibitors. A 72-hour co-treatment of AZD8055 (mTOR) or BEZ235 (mTOR-PI3K) and iBRD9 or TP472 decreased further HEK293T viability than treatments alone (Fig. 2G; Supplementary Fig. S2J).

Depletion of specific mSWI/SNF subunits alters translation

We confirmed our findings using mouse embryonic stem cells containing an auxin-dependent degron within *Smarca4*, *Arid1A*, or *Pb1* alleles, allowing a complete degradation of endogenous proteins within 2 hours of auxin treatment (14). Degradation of *Smarca4* and *Arid1A* but not *Pb1* decreased translation (Fig. 3A), suggesting the defects observed upon PFI-3 to be the consequences of SMARCA2/SMARCA4 inhibition. Depletion of *Smarca4* equally up- and down-regulated specific RNAs (14), validating potential independent roles in translation.

We then utilized HAP1-KO for PBAF (*BRD7*, *ARID2*), BAF (*ARID1A*), ncBAF (*BRD9*), and ATPases (*SMARCA2*, *SMARCA4*; Supplementary Fig. S3A). mSWI/SNF subunits presented nuclear and cytoplasmic distributions in HAP1-WT (Supplementary Fig. S3B) and their KO did not alter proliferation (Supplementary Fig. S3C). A 10-minute treatment with iBRD9 and TP472 decreased translation (Sup-

plementary Fig. S3D). Depletion of each subunit decreased translation to various degrees (Fig. 3B) but presented distinct polysome profiles. *SMARCA4*-, *ARID2*-, and *BRD7*-KO increased initiating/early and decreased late polysomes (Supplementary Fig. S3E–S3G); *SMARCA2*- and *ARID1A*-KO decreased the entire profile (Supplementary Fig. S3H and S3I); and *BRD9*-KO, albeit more variable, increased polysomes (Supplementary Fig. S3J and S3K). These distinct profiles suggest specific roles for BAF, PBAF and ncBAF in the cytoplasm as described in the nucleus. Finally, and demonstrating specificity, reexpression of GFP-SMARCA4 in *SMARCA4*-KO rescued the translational defects (Fig. 3C).

SMARCA4 pathogenic mutations decrease translation

Many mSWI/SNF cancer mutations being loss-of-function (1–3) and some heterozygous missense dominant-negative (26), we hypothesized they could alter translation. Transient overexpression of *SMARCA4* pathogenic mutations p.K785R (ATP cleft) and p.E861K (DNA groove) decreased translation without altering proliferation (Fig. 3D; Supplementary Fig. S3L).

Depletion of mSWI/SNF subunits sensitizes cells to specific translation pathway inhibitors

Because depletion of mSWI/SNF subunits decreased translation, we hypothesized it would sensitize cells to translation inhibition. *ARID2*- and *BRD7*-KO increased sensitivity to AZD8055 and BEZ235 (Fig. 3E; Supplementary Fig. S3M), while *SMARCA2*-, *SMARCA4*-, *ARID1A*-, and *BRD9*-KO did not (Fig. 3F–G; Supplementary Fig. S3N–S3O). Consistent with *ARID1A* mutations increasing cells' sensitivity to AKT inhibitors (Fig. 1A), *ARID1A*-KO sensitized cells to these inhibitors (Fig. 3H). Therefore, depletion of mSWI/SNF subunits creates a vulnerability to specific inhibitors.

PBAF-specific subunits expression is highly altered in breast cancers

Several mSWI/SNF subunits are cytoplasmic in tumors and altered localization could be useful markers (11–13). While primarily considered tumor suppressors, evidence starts to shed light on potential oncogenic roles. For example, *SMARCA4* is likely an oncogene in breast cancer (27). Mis-expression or localization not being necessarily associated with genomic alteration, we evaluated mSWI/SNF subunits in breast cancer by IHC. Mutations in the PBAF-specific subunits *ARID2* and *Pb1* being less frequent in breast cancers than the BAF-specific *ARID1A* and *ARID1B* (1, 3), we investigated expression of PBAF subunits.

PB1 presented various levels of nuclear expression in normal breast epithelium. Forty-one percent of cases presented a strong and 22% a weak cytoplasmic expression, and 30% a loss of expression (Fig. 4A; Supplementary Fig. S4A).

BRD7 presented an overall cytoplasmic with a weak nuclear expression in less than 50% of normal breast epithelium. Sixty-eight percent of cases exhibited increased nuclear and cytoplasmic expression and 16% increased cytoplasmic (Fig. 4B; Supplementary Fig. S4A).

ARID2 resembled BRD7 in normal breast epithelium. Thirty-one percent of cases presented increased nuclear expression, 26% increased cytoplasmic, 11% increased cytoplasmic and nuclear, and 12% cytoplasmic loss (Fig. 4C; Supplementary Fig. S4A).

All considered, most cases presented an increase in PBAF subunits expression. Of note, some patients presented both increased and lost expression and/or variation in compartmental distribution across different samples, highlighting the heterogeneity between primary, recurrent, and metastatic samples (Supplementary Fig. S4B).

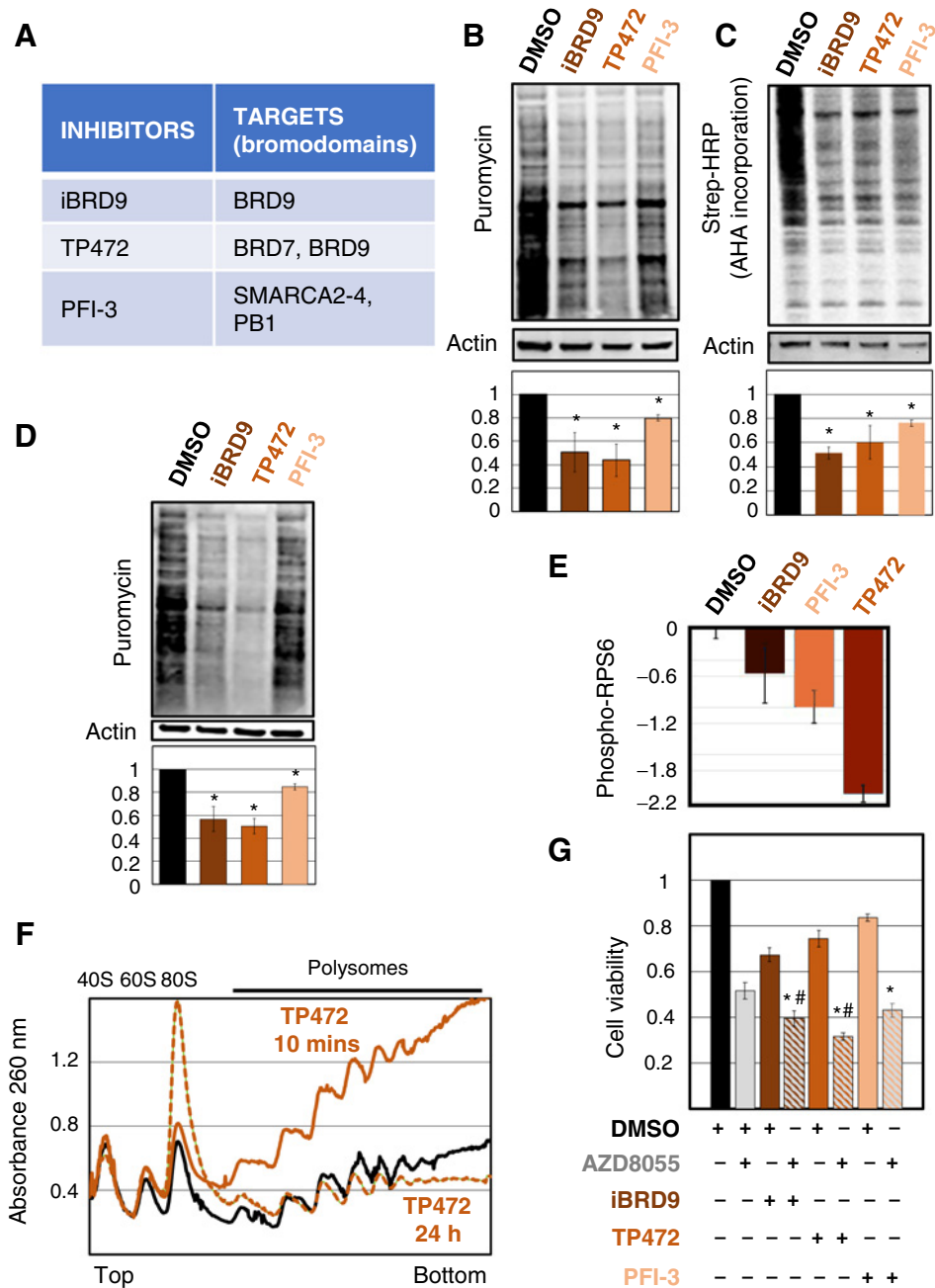


Figure 2. mSWI/SNF inhibition inhibits translation. **A**, mSWI/SNF inhibitors and targets. **B**, Puromycin incorporation assays in HEK293T treated for 24 hours. **C**, AHA incorporation assays in HEK293T treated for 24 hours. **D**, Puromycin incorporation assays in HEK293T treated for 10 minutes. **E**, Phospho-RPS6 detected by SOM₃B in HEK293T treated for 10 minutes. **F**, HEK293T polysome profiles treated for 24 hours (dotted brown) and 10 minutes (brown). **G**, Cell viability assays in HEK293T treated for 72 hours. *, to mSWI/SNF inhibitor; #, to AZD8055. h, hours; mins, minutes.

Breast cancer specimens predominantly gain SMARCA4 and lose SMARCA2

We then assessed both ATPases. As previously reported, SMARCA2 exhibited moderate nuclear expression in approximately 50% of normal breast epithelium (28). Sixty-one percent of cases demonstrated loss of SMARCA2, 9% a concomitant increased cytoplasmic, 11% increased nuclear and cytoplasmic, and 7% increased cytoplasmic only (Fig. 4D).

SMARCA4 was very minimally expressed in normal breast epithelium, with occasional cells presenting nuclear expression (28). Fifty-one percent of breast cancer cases presented increased nuclear and cytoplasmic SMARCA4 and 18% a weak cytoplasmic expression that could be considered as background (a potential limitation of IHC; Fig. 4E; Supplementary Fig. S4A). Five cases (11%) harbored a SMARCA4 mutation, three of which with increased expression (Supplementary Fig. S4C).

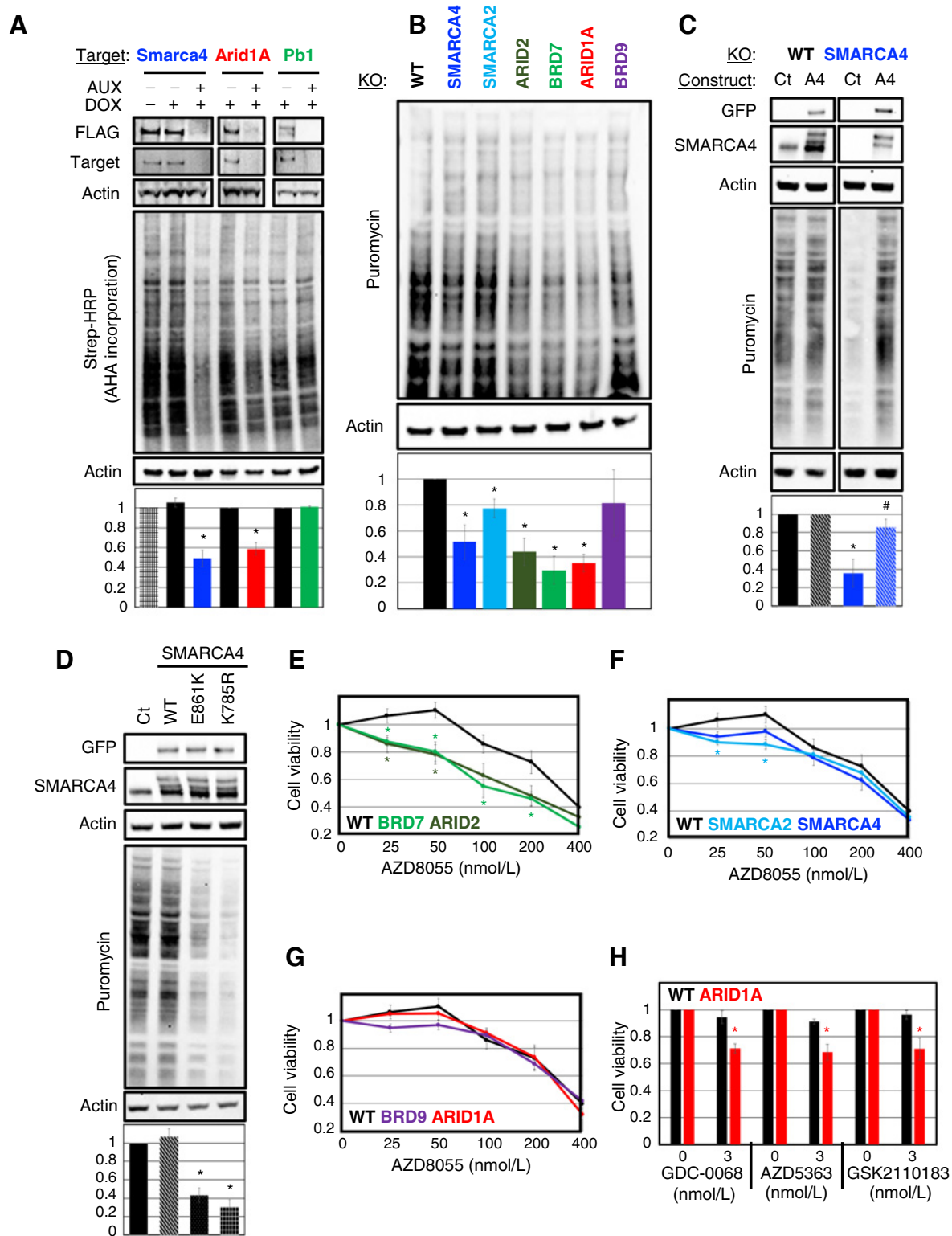


Figure 3. mSWI/SNF depletion inhibits translation and sensitizes cells to translation pathway inhibitors. **A**, AHA incorporation assays in ES cells treated with doxycycline (DOX; Fbox induction) and 2 hours of auxin (AUX; degradation of FLAG-Smarca4, -Arid1A, and -Pb1). **B**, Puromycin incorporation assays in HAP1-KO. **C**, Puromycin incorporation assays in HAP1-WT and HAP1-SMARCA4-KO upon overexpression of GFP-Ct or GFP-SMARCA4. **D**, Puromycin incorporation assays in HAP1-WT overexpressing GFP-SMARCA4-mutants. **E-H**, Cell viability assays in HAP1 treated for 72 hours. *, to WT.

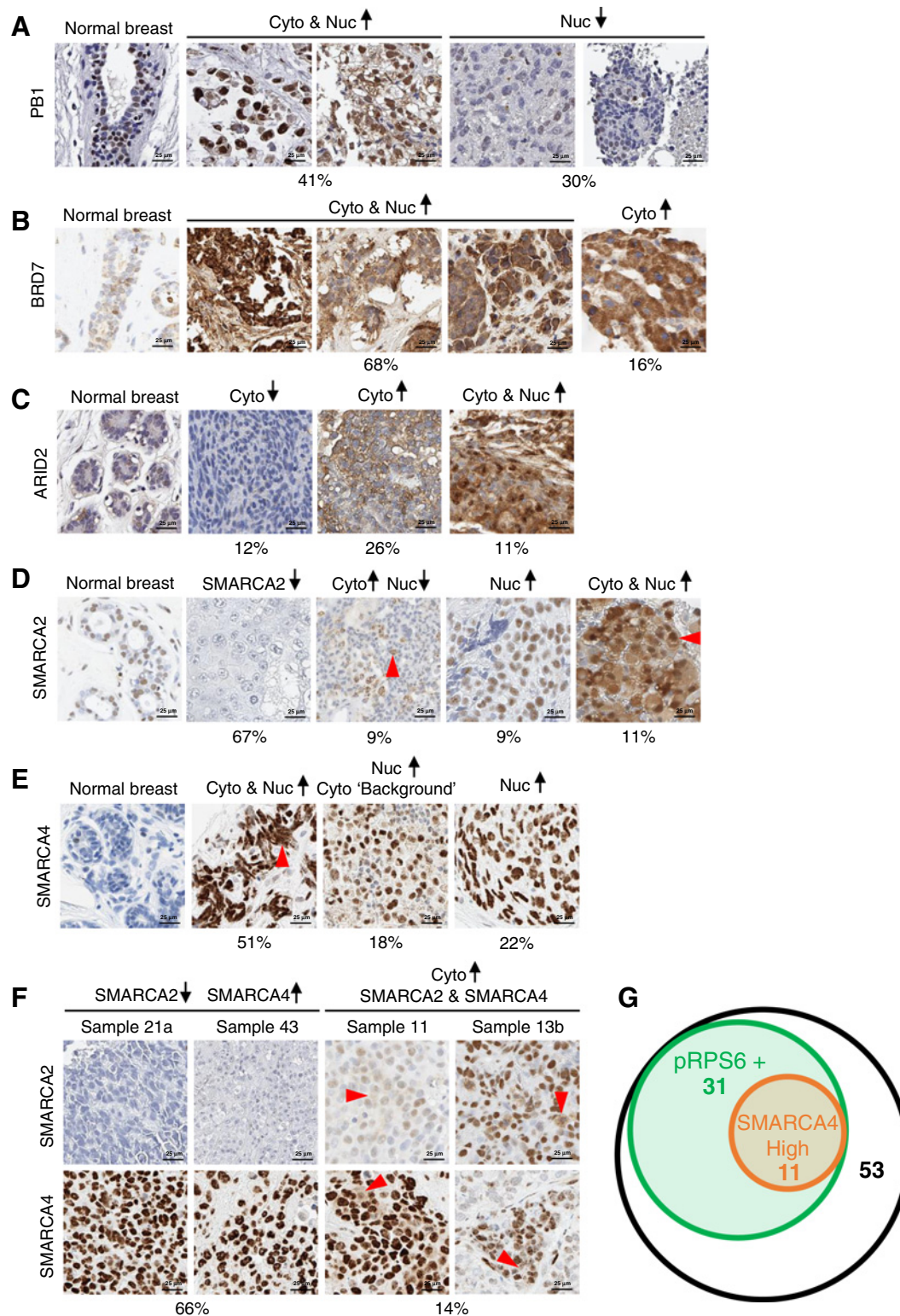


Figure 4. mSWI/SNF subunits expression and subcellular localization are altered in breast cancers. **A-F**, 20× breast cancers IHC of PB1 (**A**), BRD7 (**B**), ARID2 (**C**), SMARCA2 (**D**), SMARCA4 (**E**), and SMARCA2 and SMARCA4 (**F**). Cyto, cytoplasmic; Nuc, nuclear. **G**, Representations of cores presenting phospho-RPS6 and high cytoplasmic SMARCA4. Numbers of cores in each group are reported.

Taken together, 14% of cases presented an increased cytoplasmic SMARCA4 and SMARCA2, and 66% an increased expression of SMARCA4 with a loss of SMARCA2, suggesting a swap of ATPases within mSWI/SNF complexes (Fig. 4F).

Cytoplasmic SMARCA4 correlates with phosphorylated RPS6 and disease progression

Because 10 minutes of mSWI/SNF inhibition decreased phospho-RPS6 (Fig. 2E), we examined its presence in our breast cancer specimens. Each core with high cytoplasmic SMARCA4 presented phospho-RPS6 (Fig. 4G; Supplementary Table S2), consistent with a correlation between cytoplasmic SMARCA4 and levels of translation in breast cancer.

Finally, assessment of clinical information suggested a correlation between cytoplasmic SMARCA4 and breast cancer progression: SMARCA4 presented a high cytoplasmic expression in 7% of primary tumors, 31% of local recurrences, and 42% of metastases (Supplementary Table S1).

Discussion

This study reports the cytoplasmic presence of mSWI/SNF and its implication in translation. KO of each tested subunit decreased translation, but cell sensitivity to mTOR-PI3K inhibition increased upon depletion of PBAF-specific subunits. This could reflect complexes' specific roles in translation. Confirming a potential specificity, PBAF-KOs presented identical polysome profiles. SMARCA4-KO polysome profiles resembled PBAF-KOs and SMARCA2-KO resembled BAF-KO; future studies will determine if cytoplasmic complexes involve specific ATPases, in contrast to the nucleus (21).

mSWI/SNF-mutated cancer cells were genetically dependent to translation factors and sensitive to translation pathway inhibitors. This could be used as a clinical strategy, such as PARP inhibitors for BRCA-deficient cancers (29). However, some subunits such as BRD9 did not present such dependency even though iBRD9 decreased translation. Only specific mutations (i.e., bromodomain) could increase sensitivity to translation pathway inhibitors and be missed when considering all mutations. A systematic study of each subunit's cancer alterations will be necessary to assess consequences on translation and sensitivity to translation pathway inhibitors.

Large-scale sequencing studies revealed the cooccurrence of mutations in PI3K and mSWI/SNF, and a cooperative mechanism suggested (2, 3). While biologically this cooccurrence is not understood, roles for mSWI/SNF in translation could be relevant. The decreased translation upon mSWI/SNF-inactivating mutations could need the counteraction of increased translation through *PI3K*-activating or *PTEN*-inactivating mutations (3). Altering the translation of specific mRNAs is another route to enable a selective advantage to cancer cells. We do not observe any association between *PI3K* mutations and mSWI/SNF altered expression/localization in breast cancers. SMARCA4 was overexpressed in more than 90% of cases, confirming a potential oncogene and its low expression as a favorable outcome (3, 27). On the contrary, SMARCA2 expression was extensively lost. It will be interesting to determine if such cases are more sensitive to translation inhibitors, especially when SMARCA4 is not overexpressed and/or mutated. Furthermore, some cases exhibited loss of PBAF subunits, which could sensitize to mTOR/PI3K inhibitors. Finally, we also observed several cases with exclusive gain in cytoplasmic expression or opposite changes within different compartments. The consequences of differences in subcellular functions could

have great potential for the discovery of therapeutically targetable events.

Our study supports a direct role for mSWI/SNF complexes in translation, however, we cannot completely exclude that other mSWI/SNF functions are important. Transcription and translation being intertwined, it is challenging to experimentally separate one from the other. Furthermore, mSWI/SNF complexes could regulate the transcription and translation of identical mRNAs. However, understanding the direct and indirect functions of mSWI/SNF in translation is essential to understanding the consequences of their cancer alterations.

In summary, we underscore that mSWI/SNF cancer mutations render cells sensitive to translation pathway inhibitors and genetically dependent to translation factors. We further demonstrate mSWI/SNF interacts with the translation machinery and its inhibition, depletion, and cancer mutations decrease global translation. Overall, this study highlights that considering unappreciated functions for chromatin remodelers could be essential to the discovery of new therapeutic strategies.

Authors' Disclosures

G.R. Crabtree reports personal fees and other support from Foghorn Therapeutics outside the submitted work. C. Van Rechem reports grants from The Children's Cancer Research Fund, The Stanford Women's Cancer Center and the Stanford Cancer Institute (Stanford, CA), The Jacob Churg Award, and grants from The Weintz Family COVID-19 Research Fund during the conduct of the study. No disclosures were reported by the other authors.

Authors' Contributions

L. Ulicna: Conceptualization, investigation, writing–review and editing. **S.C. Kimmey:** Investigation, writing–review and editing. **C.M. Weber:** Resources, investigation, writing–review and editing. **G.M. Allard:** Investigation. **A. Wang:** Resources, data curation, supervision, funding acquisition, writing–review and editing. **N.Q. Bui:** Resources, formal analysis, supervision, writing–review and editing. **S.C. Bendall:** Resources, supervision, funding acquisition, writing–review and editing. **G.R. Crabtree:** Conceptualization, resources, supervision, writing–original draft, writing–review and editing. **G.R. Bean:** Resources, data curation, supervision, writing–review and editing. **C. Van Rechem:** Conceptualization, formal analysis, supervision, writing–original draft, writing–review and editing.

Acknowledgments

C. Van Rechem was supported by the Stanford Women's Cancer Center and the Stanford Cancer Institute, the Weintz Family COVID-19 Research Fund, the Jacob Churg Award, and the Children's Cancer Research Fund. G.R. Crabtree was supported by the Howard Hughes Medical Institute, grants from the NIH (grant nos. CA163915 and NS046789), and a grant from the Department of Defense, Breast Cancer Research fund. C.M. Weber was supported by a grant from GSK, Sir James Black Fellowship. S.C. Kimmey and S.C. Bendall received support from the NIH (grant no. T32GM007276 to S.C. Kimmey; grant nos. 1DP2OD022550-01, 1R01AG056287-01, 1R01AG057915-01, and 1U24CA224309-01 to S.C. Bendall). This work was supported in part by NIH P30 CA124435 utilizing the Stanford Cancer Institute Proteomics/Mass Spectrometry Shared Resource, Vincent Coates Foundation Mass Spectrometry Laboratory (RRID: SCR_017801).

The authors thank Drs. Joshua Black and Johnathan Whetstine for helpful discussions, and Ellen Gomulia and Ivy Mangonon for assistance with SMARCA4 IHC.

Note

Supplementary data for this article are available at Cancer Research Online (<http://cancerres.aacrjournals.org/>).

Received April 29, 2021; revised January 10, 2022; accepted June 15, 2022; published first June 24, 2022.

References

- Hodges C, Kirkland JG, Crabtree GR. The many roles of BAF (mSWI/SNF) and PBAF complexes in cancer. *Cold Spring Harb Perspect Med* 2016;6.
- Kadoch C, Crabtree GR. Mammalian SWI/SNF chromatin remodeling complexes and cancer: Mechanistic insights gained from human genomics. *Sci Adv* 2015;1:e1500447.
- Mittal P, Roberts CWM. The SWI/SNF complex in cancer - biology, biomarkers and therapy. *Nat Rev Clin Oncol* 2020;17:435–48.
- Sima X, He J, Peng J, Xu Y, Zhang F, Deng L. The genetic alteration spectrum of the SWI/SNF complex: the oncogenic roles of BRD9 and ACTL6A. *PLoS One* 2019;14:e0222305.
- Agarwal R, Chan Y-C, Tam CS, Hunter T, Vassiliadis D, Teh CE, et al. Dynamic molecular monitoring reveals that SWI-SNF mutations mediate resistance to ibrutinib plus venetoclax in mantle cell lymphoma. *Nat Med* 2019;25:119–29.
- Manning BJ, Peterson CL. Direct interactions promote eviction of the Sir3 heterochromatin protein by the SWI/SNF chromatin remodeling enzyme. *Proc Natl Acad Sci* 2014;111:17827–32.
- Kapoor P, Bao Y, Xiao J, Luo J, Shen J, Persinger J, et al. Regulation of Mec1 kinase activity by the SWI/SNF chromatin remodeling complex. *Genes Dev* 2015;29:591–602.
- Stanton BZ, Hodges C, Calarco JP, Braun SMG, Ku WL, Kadoch C, et al. Smarca4 ATPase mutations disrupt direct eviction of PRC1 from chromatin. *Nat Genet* 2016;49:ng.3735.
- Park SW, Herrema H, Salazar M, Cakir I, Cabi S, Sahin FB, et al. BRD7 regulates XBP1s' activity and glucose homeostasis through its interaction with the regulatory subunits of PI3K. *Cell Metab* 2014;20:1088.
- Lee JH, Chang SH, Shim JH, Lee JY, Yoshida M, Kwon H, et al. Cytoplasmic localization and nucleo-cytoplasmic shuttling of BAF53, a component of chromatin-modifying complexes. *Mol Cells* 2003;16:78–83.
- Bilodeau S, Vallette-Kasic S, Gauthier Y, Figarella-Branger D, Brue T, Berthelet F, et al. Role of Brg1 and HDAC2 in GR trans-repression of the pituitary POMC gene and misexpression in cushing disease. *Genes Dev* 2006;20:2871–86.
- Fukuoka J, Fujii T, Shih JH, Dracheva T, Meerzaman D, Player A, et al. Chromatin remodeling factors and BRM/BRG1 expression as prognostic indicators in non-small cell lung cancer. *Clin Cancer Res* 2004;10:4314–24.
- Animireddy S, Kavadiyula P, Kotapalli V, Gowrishankar S, Rao S, Bashyam MD. Aberrant cytoplasmic localization of ARID1B activates ERK signaling and promotes oncogenesis. *J Cell Sci* 2021;134:jcs251637.
- Weber CM, Hafner A, Kirkland JG, Braun SMG, Stanton BZ, Boettiger AN, et al. mSWI/SNF promotes polycomb repression both directly and through genome-wide redistribution. *Nat Struct Mol Biol* 2021;28:501–11.
- Van Rechem C, Ji F, Mishra S, Chakraborty D, Murphy SE, Dillingham ME, et al. The lysine demethylase KDM4A controls the cell-cycle expression of replicative canonical histone genes. *Biochim Biophys Acta Gene Regul Mech* 2020;1863:194624.
- Van Rechem C, Black JC, Boukhali M, Aryee MJ, Gräslund S, Haas W, et al. Lysine demethylase KDM4A associates with translation machinery and regulates protein synthesis. *Cancer Discov* 2015;5:255–63.
- Kimmy SC, Borges L, Baskar R, Bendall SC. Parallel analysis of tri-molecular biosynthesis with cell identity and function in single cells. *Nat Commun* 2019;10:1185.
- Schmidt EK, Clavarino G, Ceppi M, Pierre P. SUNSET, a nonradioactive method to monitor protein synthesis. *Nat Methods* 2009;6:275–7.
- Yu C, Mannan AM, Yvone GM, Ross KN, Zhang Y-L, Marton MA, et al. High-throughput identification of genotype-specific cancer vulnerabilities in mixtures of barcoded tumor cell lines. *Nat Biotechnol* 2016;34:419–23.
- McFarland JM, Ho ZV, Kugener G, Dempster JM, Montgomery PG, Bryan JG, et al. Improved estimation of cancer dependencies from large-scale RNAi screens using model-based normalization and data integration. *Nat Commun* 2018;9:4610.
- Mashtalir N, D'Avino AR, Michel BC, Luo J, Pan J, Otto JE, et al. Modular organization and assembly of SWI/SNF family chromatin remodeling complexes. *Cell* 2018;175:1272–88.
- Fuchs G, Voichek Y, Benjamin S, Gilad S, Amit I, Oren M. 4sUDRB-seq: measuring genomewide transcriptional elongation rates and initiation frequencies within cells. *Genome Biol* 2014;15:R69.
- Olofsson S-O, Boström MK, Carlsson P, Borén J, Wettsten M, Bjursell G, et al. Structure and biosynthesis of apolipoprotein B. *Am Heart J* 1987;113:446–52.
- Pyronnet SP, Dostie JE, Sonenberg N. Suppression of cap-dependent translation in mitosis. *Genes Dev* 2001;15:2083–93.
- Bohlen J, Roiuk M, Teleman AA. Phosphorylation of ribosomal protein S6 differentially affects mRNA translation based on ORF length. *Nucleic Acids Res* 2021;49:13062–74.
- Hodges HC, Stanton BZ, Cermakova K, Chang C-Y, Miller EL, Kirkland JG, et al. Dominant-negative SMARCA4 mutants alter the accessibility landscape of tissue-unrestricted enhancers. *Nat Struct Mol Biol* 2018;25:61–72.
- Wu Q, Lian JB, Stein JL, Stein GS, Nickerson JA, Imbalzano AN. The BRG1 ATPase of human SWI/SNF chromatin remodeling enzymes as a driver of cancer. *Epigenomics* 2017;9:919–31.
- Reisman DN, Sciarrotta J, Bouldin TW, Weissman BE, Funkhouser WK. The expression of the SWI/SNF ATPase subunits BRG1 and BRM in normal human tissues. *Appl Immunohistochem Mol Morphol* 2005;13:66–74.
- Dziadkowiec KN, Gasiorowska E, Nowak-Markwitz E, Jankowska A. PARP inhibitors: review of mechanisms of action and BRCA1/2 mutation targeting. *Prz Menopauzalny* 2016;15:215–9.